The Pierre Auger Observatory status

R. Assiro[2], C. Bleve [1,2], G. Cataldi[2], M. R. Coluccia[1,2], A. Corvaglia[2], P. Creti[2], S. D'Amico[2,3] G. Fiore[2], A. Innocente[2],I. De Mitri[1,2], G. Marsella[1,2], D. Martello[1,2], A. Miccoli[2], L.Perrone[1,2], C. Pinto[1,2], V. Scherini[2], F. Strafella[1,2] and the Pierre Auger Collaboration[4]

[1] Dipartimento di Matematica e Fisica "Ennio De Giorgi", Università del Salento, Italy
[2] Istituto Nazionale di Fisica Nucleare sez. di Lecce, Italy
[3] Dipartimento di Ingegneria dell'Innovazione Università del Salento, Italy
[4] http://www.auger.org/archive/authors_2016_06.html

1. Introduction

The nature and the origin of ultra-high energy cosmic rays above 10^{17} are still unknown, even if in the last decade measurements have shed light on these puzzling questions. Understanding the sources, nature and propagation properties of UHECRs is one of the key questions in astroparticle physics. From the experimental point of view, their study can be performed indirectly, by using the extensive air showers (EASs) they produce by interacting with the nuclei of the molecules that compose the atmosphere of the Earth.

Anyway, the all particle spectrum by itself cannot provide sufficient discrimination between the different astrophysical hypotheses, and the determination of the primary composition is mandatory to reach any reliable conclusion.

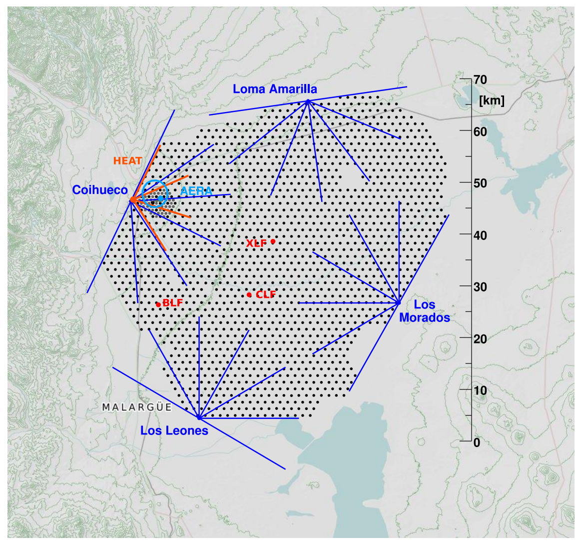

Figure 1. The Auger Observatory layout. Each dot corresponds to one of the 1660 surface detector stations. The four fluorescence detector sites are shown, each with the field of view of its six telescopes. The Coihueco site hosts three extra high elevation (HEAT) telescopes. The 750 m array is located a few kilometers from Coihueco.

2. The Pierre Auger Observatory

The Pierre Auger Observatory [1] with its 3000 km^2 of instrumented surface, brings unique capabilities to the UHECR study. The Observatory is located in the province of Mendoza (Argentina) near the city of Malargue in a vast high plain. It is the world's largest cosmic ray observatory. The Observatory consists of an array (SD) of 1600 water-Cherenkov particle detector stations (WCD) overlooked by 24 air fluorescence telescopes (FD). In addition, three high elevation fluorescence telescopes (HEAT) overlook a surface of 23.5 km^2 where 61 additional WCDs (Infill) are installed (see figure 1).

Each WCD of the surface detector is a water-Cherenkov detector which samples the particle content of the EAS falling on the array. The WCD consists of a 12,000 liter polyethylene water tank containing a sealed laminated polyethylene liner with a reflective inner surface. Cherenkov light from the passage of charged particles is collected by three 230 mm photomultiplier tubes (PMTs) that look through windows of clear polyethylene into highly purified water. The WCD is self contained. A solar power system provides power for the PMTs and electronics package. The electronics package, consisting of a processor, GPS receiver, radio transceiver and power controller, is mounted on the container. The WCD stations are placed on a triangular grid with 1500 m spacing (SD-1500).

The 24 telescopes of the FD overlook the SD array from four sites: Los Leones, Los Morados, Loma Amarilla and Coihueco [1] (see figure 1).

Six independent telescopes are located at each FD site in a clean climate-controlled building. A single telescope has a field of view of $30^{\circ} \times 30^{\circ}$ in azimuth and elevation, with a minimum elevation of 1.5° above the horizon. The telescopes face towards the interior of the array so that the combination of the six telescopes provides 180° coverage in azimuth.

Three additional fluorescence telescopes (HEAT) with an elevated field of view were built at the FD site at Coihueco. These telescopes are very similar to the original fluorescence telescopes but are tilted by 29° upward. These three telescopes work independently of other FD sites and form the "fifth site" of the Observatory. The HEAT telescopes were designed to cover the elevation range from 30° to 58°, which lies above the field of view of the other FD telescopes. The HEAT telescopes allow a determination of the cosmic ray spectrum and X_{max} distributions in the energy range from below the second knee up to the ankle.

The Infill array consists of a denser WCD array with 750 m spacing (SD-750) nested within the 1500 m array covering a surface of 23.5 km^2. The area is centered 6 km away from the Coihueco fluorescence site. The Infill array is fully efficient from 3×10^{17} eV onwards for air showers with zenith angle $\leq 55^{\circ}$.

On-line and long-term performance of the detectors and data quality are monitored continuously, and a set of high-quality devices installed in the Observatory monitors the atmospheric conditions during operation.

High-quality data have been collected continuously for about ten years, with a SD annual exposure of 5500 km^2 sr yr. The longitudinal profile reconstructed by the FD is providing a nearly calorimetric measurement of the primary energy, with total systematic uncertainty of 14% [2]. From the shower lateral distribution reconstructed using the WCD signals, a SD energy estimator is inferred. A high-quality subset of hybrid events recorded by both the SD and the FD is used to calibrate the SD energy estimator with the FD energy measurement, hence providing an almost model-independent energy calibration.

3. The Spectrum

The Pierre Auger Observatory has collected data of excellent quality for more than 10 years, which has already led to a measurement of the flux of UHECRs above 3×10^{17} eV with unprecedented statistics.

The events used for the determination of the energy spectrum consist of 4 different sets of data:

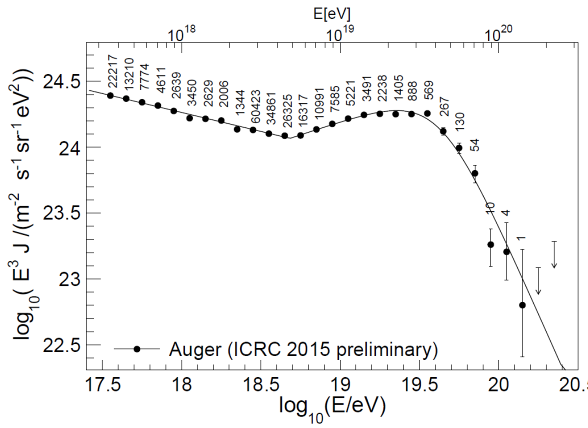

Figure 2. The combined energy spectrum measured by the Auger Observatory, fitted with a flux model. The data points include only the statistical uncertainties. For each data point is reported the number of events.

the SD-1500 vertical events with zenith angle up to 60°, the SD-1500 inclined events with zenith angle between 60° and 80°, the SD-750 vertical events and the hybrid events. The hybrid set of data contains events detected simultaneously by the fluorescence telescopes and by at least one WCD.

The first step in the procedure used for the determination of the spectrum is the evaluation of the energy of the events. The FD allows the measurement of the electromagnetic energy released by the shower in the atmosphere as a function of the atmospheric depth. The total primary energy is then derived by integrating this longitudinal profile over the depth range and adding an estimate of the so-called invisible energy carried into the ground by high-energy muons and neutrinos.

The SD samples the shower particles that reach the ground. The intensities of the signals registered in the WCD are used to quantify the shower size and the impact point of the shower axis on the ground.

The absolute calibration of the SD sets of data is inferred from a high-quality subset of hybrid events (full details in [3, 4, 5]).

The final step in the procedure used for the determination of the energy spectrum is a precise evaluation of the exposure. Above the energy for full detector efficiency, the calculation of the SD exposure is based on the determination of the geometrical aperture of the array for the corresponding zenith-angle interval and of the observation time. The choice of a fiducial trigger based on active hexagons allows one to exploit the regularity of the array, and to compute the aperture simply as the sum of the areas of all active hexagons. The calculation of the exposure for the hybrid set of data is more complex. It relies on a detailed time-dependent Monte Carlo simulation which exactly reproduces the data taking conditions and includes the response of the hybrid detector [6].

The energy spectrum reported in figure 2 has been obtained by combining the four independent sets of data. They are combined using a method that takes into account the systematic uncertainties of the individual measurements (see details in [7]).

The characteristic features of the combined energy spectrum, shown in figure 2, have been quantified by fitting a model that describes a spectrum by a power-law below the ankle $J(E) = J_0(E/E_{ankle})^{\gamma_1}$ and power-law with a smooth suppression at the highest energies:

$$J(E) = J_0 \left(\frac{E}{E_{ankle}}\right)^{-\gamma_2} \left[1 + \left(\frac{E_{ankle}}{E_s}\right)^{\Delta\gamma}\right] \times \times \left[1 + \left(\frac{E}{E_s}\right)^{\Delta\gamma}\right]^{-1}$$

Here, γ_1 and γ_2 are the spectral indexes below and above the ankle energy E_{ankle} respectively, E_s is the energy at which the differential flux falls to one-half of the value of the power-law extrapolation from the intermediate region, $\Delta\gamma$ gives the increment of the spectral index beyond the suppression region, and J_0 is the normalization of the flux, taken as the value of the flux at $E = E_{ankle}$.

The result of the best fit is shown in figure 2 and the corresponding parameters are presented in Table 1, quoting both statistical and systematic uncertainties.

The energy spectrum can also be exploited to study the distribution of cosmic-ray sources by searching for a flux variation with declination (δ) of the incoming directions. This study is of particular interest to the discussion of the difference seen in the suppression region between the spectra measured by Auger and by the Telescope Array experiment [8], which, despite being still compatible within the quoted systematic uncertainties of both experiments, is not understood so far.

4. Mass Composition

Different observables can be used to obtain information on the primary composition, the most direct of which is the depth of maximum development of the longitudinal shower profile (X_{max}), measured by the FD. X_{max} is related to the depth of the first interaction of the primary and to the subsequent development of the shower. For this reason, the interpretation in terms of composition is complicated by the large uncertainties in the hadronic interaction models used in the simulations (see [9] these proceedings). The average of the X_{max} for different energies of the primary and its RMS can be directly compared to the predictions of air shower simulations using recent post-LHC hadronic interaction models, as shown in figure 3.

Our measurements are clearly at variance with model predictions for pure composition; assuming no change in hadronic interactions at these energies, they point to a composition getting heavier above the ankle.

5. Search for Anisotropy

Complementary to the spectrum and mass measurements are the searches for anisotropy. Due to the energy losses during propagation through the Cosmic Microwave Background (CMB) the position of the astrophysical sources of UHECRs should be relatively nearby, which in case of light nuclei with $E > 40$ EeV would result in anisotropies in arrival directions, reflecting the distribution of the nearby extragalactic matter. For protons of this energy, deflections in the encountered magnetic fields are quite small, while for nuclei of atomic number Z they are Z times larger.

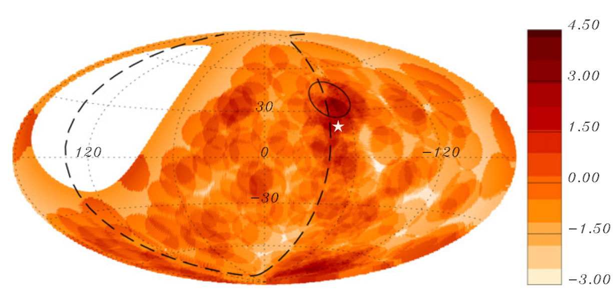

Figure 4. Map of the Li-Ma significances of overdensities in windows of 12^o for events with $E \geq 54$ EeV. Dashed line: Super-Galactic Plane. White star: Centaurus A

In the more recent analysis [10] 602 events have been selected with energy above 40 EeV recorded in the 10 years of operation of the Pierre Auger Observatory in the declination range of

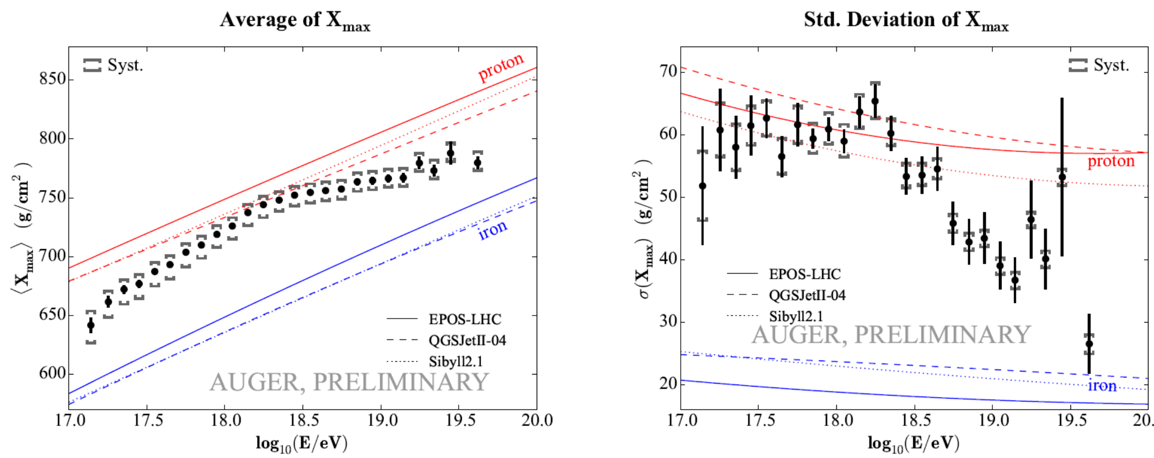

Figure 3. Average and RMS of the X_{max} compared to the model predictions for an all-proton and an all-iron composition.

Table 1
Best-fit parameters for the combined energy spectrum, statistical and systematic uncertainties being reported.

J_0 [eV^{-1} km^{-2} sr^{-1} yr^{-1}]	E_{ankle} [EeV]	E_s [EeV]
$(3.30 \pm 0.15 \pm 0.20) \times 10^{-19}$	$4.82 \pm 0.07 \pm 0.8$	$42.1 \pm 1.7 \pm 7.6$
γ_1	γ_2	$\Delta\gamma$
$3.29 \pm 0.02 \pm 0.05$	$2.69 \pm 0.02 \pm 0.1$	$3.14 \pm 0.2 \pm 0.4$

-90^o to $+45^o$. Various kinds of tests were performed to search for anisotropy above a certain threshold in various angular windows as well as auto-correlations of arrival directions. Correlations were also sought with catalogs of plausible candidates of UHECR sources. The two largest departures from isotropy are found above 58 EeV and correspond to the direction within 15^o of Centaurus A, the closest radio-loud AGN, and to the arrival direction within 18^o of Swift-BAT AGNs closer than 130 Mpc and brighter than 10^{44} erg s^{-1}. None of the excesses is statistically significant (see figure 4). Therefore, either the primaries are light nuclei and the sources are numerous or the isotropy is caused by large deflections of nuclei with larger Z. A full sky study of arrival directions has been performed in collaboration with Telescope Array and IceCube [11]. The study included 231 events with energy above 52 EeV from the Pierre Auger Observatory, 87 events with energy above 57 EeV from the Telescope Array and the very high energy neutrinos from IceCube. No correlations at the discovery level were found.

Large scale anisotropy can reveal the effects of the global distribution of sources and the collective motion of cosmic rays. Using events recorded by the SD from 2004 January 1 to 2013 December 31 an analysis [12] was performed including also inclined events, reaching a coverage of about 85% of the sky. The set of data consists of about 70 000 events with energies above 4 EeV, where full efficiency for inclined events is attained. Two Rayleigh analyses were performed, in right ascension and azimuth angles in two energy bins, 4-8 EeV and above 8 EeV. While the lower energy bin does not show any significant departure from isotropy of arrival directions, a dipole was found at energies above 8 EeV of an amplitude 0.073 ± 0.015 pointing to $(\alpha, \delta) = (-95^o \pm 13^o, -39^o \pm 13^o)$. A sky map of the flux in equatorial coordinates is shown in figure 5. Observation of dipolar amplitudes in arrival directions of UHECRs is consistent with expectations for heavier nuclei suggested by the X_{max} distributions.

6. Astrophysical Interpretation

The accurate measurement of the spectrum, the results from the study of the mass composition and the distribution of the arrival directions of the primaries, gives the possibility to infer some hypothesis on the origin and propagation of UHECRs [13].

Assuming that all UHECR sources emit

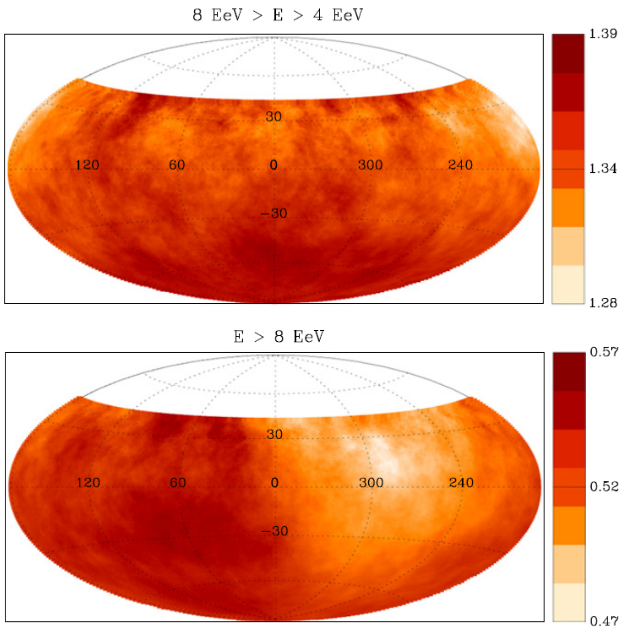

Figure 5. Sky map of flux for two bins of energy in $km^{-2}yr^{-1}sr^{-1}$ units. The data are smoothed in angular windows of 45^o. (Galactic coordinates)

hydrogen-1, helium-4, nitrogen-14 and iron-56 with a broken exponential rigidity cutoff, it is possible to infer some characteristics of the acceleration sites and put some constraint on the propagation process. Unfortunately, with the publicly available codes that simulate the propagation of the UHECRs from the sources to the Earth [14, 15], it is not possible to take into account the anisotropy study in the global fit procedure. For this reasons all the UHECR sources are assumed identical and uniformly distributed in the near universe. In this analysis both the propagation codes and different sets of parameters for the propagation processes are taken into account. The interaction of the primary with the atmosphere has been simulated with three different interaction codes [18,**?**, **?**]. The detector resolutions and acceptances are included. The data we attempt to fit consist of 15 measurements of the UHECR energy spectrum and 110 non-zero measurements of the X_{max} distribution. The free parameters of the fit are: the injection normalization factor J_0, the injection spectral index γ, the cutoff rigidity R_{cut} and the fractions of the different primaries at injection (three free parameters). In total there are 125 non-zero data points and 6 free parameters.

The minimization of the χ^2 distribution identifies a best fit solution for $\gamma = 0.94^{+0.09}_{-0.10}$ and $R_{cut} = 10^{18.67\pm0.03}$ with $\chi^2/d.o.f. = 178.5/119$. A second minimum in the χ^2 distribution is found at $\gamma = 2.03$ and $R_{cut} = 10^{19.84}$ for $\chi^2/d.o.f. = 235/119$ [13]. The corresponding simulated spectra and the mean and variance of the simulated X_{max} distributions are shown in figure 6 for the two solutions. The best fit solution of the Auger data predicts a very hard injection spectrum ($\gamma < 1$) and a rigidity cutoff that implies that the UHECR flux above $10^{19.5}$ eV is mostly limited by the maximum energy at the sources. The second minimum ($\gamma \sim 2$) with its larger rigidity cutoff is more in line with the standard models for UHECR acceleration.

In this analysis, the spectrum measured with high statistics and with different combinations and configurations of detectors has been combined with the mass composition sensitive parameters detected only with the fluorescence detector in a limited range of energy and with a number of events that is about 15% of the statistics collected for the spectrum. Moreover, a similar analysis limited to regions of the sky where there is an evidence for anisotropies in the cosmic ray flux is desirable. This is not possible with the mass sensitive data collected only by the fluorescence detector due to the limited statistics.

REFERENCES

1. The Pierre Auger Collaboration, Nucl. Instrum. Meth. **A 798**, 172 (2015)
2. V. Verzi for the Pierre Auger Collaboration, in *Proc. of ICRC 2013* (Proceedings, Rio de Janeiro Brazil, 2013) 0928
3. The Pierre Auger Collaboration, JCAP **1408**, 08, 019 (2014)
4. R. Pesce for the Pierre Auger Collaboration, in *Proc. of ICRC 2011* (Proceedings, Beijing China, 2011) 0214
5. D. Ravignani for the Pierre Auger Collaboration, in *Proc. of ICRC 2013* (Proceedings, Rio de Janeiro Brazil, 2013) 0693
6. The Pierre Auger Collaboration, Astropart. Phys. **34**, 368 (2011)
7. I. Valiño for the Pierre Auger Collaboration, in *Proc. of ICRC 2015* (Proceedings of Science, The Hague Netherlands, 2015)
8. Pierre Auger and Telescope Array Collaborations, I.C. Maris et al., in *Proc. of UHECR2014* (Utah USA, 2015)
9. A. Yushkov for the Pierre Auger Collaboration, *in these proceedings*
10. The Pierre Auger Collaboration, The Astrophysical Journal **804 (1)**, 15 (2015)
11. IceCube, Telescope Array and Pierre Auger

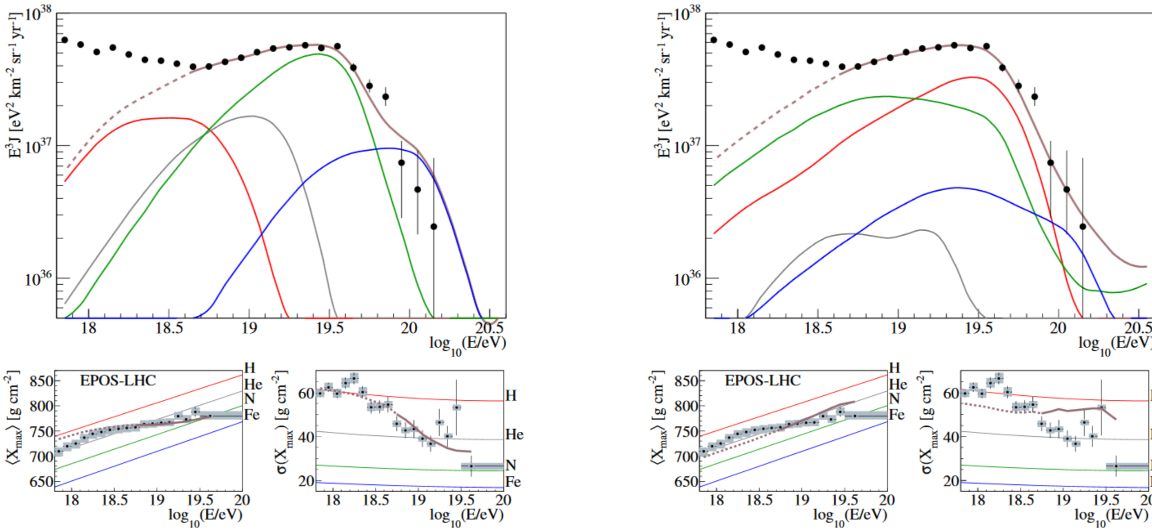

Figure 6. Top: simulated energy spectrum of UHECRs (multiplied by E^3) at the top of the Earths atmosphere with the best-fit parameters (left) and the second minimum of the likelihood for $\gamma \sim 2$ (right), compared with Auger data points. Partial spectra are grouped according to the mass number as follows: A=1 (red), 2¡A¡4 (grey), 5¡A¡26 (green), 27¡A (blue), total (brown). Bottom: average and standard deviation of the X_{max} distribution as predicted in the two scenarios (brown). Pure 1 H (red), 4 He (grey), 14 N (green) and 56 Fe (blue) are shown as reference. Only the energy range where the brown lines are solid is included in the fit.

Collaborations, in *Proc. of ICRC 2015* (Proceedings of Science, The Hague Netherlands, 2015)
12. The Pierre Auger Collaboration, The Astrophysical Journal **802 (2)**, 111 (2015)
13. A. Di Matteo for the Pierre Auger Collaboration, in *Proc. of ICRC 2015* (Proceedings of Science, The Hague Netherlands, 2015) 0249
14. R. Aloisio et al., JCAP **1210**, 007 (2012)
15. E. Armengaud et al., Astropart. Phys. **42**, 463 (2007)
16. S. Ostapchenko, Phys. Rev. **D74**, 014026 (2006)
17. E.-J. Ahn et al., Phys. Rev. **D80**, 094003 (2009)
18. K. Werner, F.-M. Liu, and T. Pierog, Phys. Rev. **C74**, 044902 (2006)
19. D. Martello for the Pierre Auger Collaboration, Nucl. Instr. and Meth. **A742**, 16 (2014)